

Production of clusters in π^-N and π^-C interactions at 40 GeV/c

J. B. Singh, I. S. Mitra, and P. M. Sood

Physics Department, Panjab University, Chandigarh-160014, India

(Received 6 October 1981)

Cluster production has been studied in π^-N and π^-C interactions at 40 GeV/c using a propane bubble chamber, and results obtained have been analyzed on the basis of two models which are in the framework of the multiperipheral model, one due to Snider and the other due to Quigg, Pirlä, and Thomas.

I. INTRODUCTION

Recently the idea of cluster production in the intermediate stage of multiparticle production in high-energy collisions has attained general acceptability. Therefore, in a number of recent papers, studies of the strength of correlations among the produced particles has been carried out, because this can provide information about the nature of clusters produced. Several theoretical attempts have also been made to explain particle production through the formation and decay of clusters produced in proton-nucleon interactions. There are two models which in the framework of the multiperipheral model have incorporated a cluster hypothesis, one due to Snider¹ and the other due to Quigg, Pirlä, and Thomas² (QPT). Both have used rapidity gaps for explaining the characteristics of clusters produced in hadron-nucleon interactions at high energies. However, the predictions of these models differ with each other. In order to find out the behavior of clustering in the collision of pion with nucleon as well as nucleus, we have analyzed events produced in a propane bubble chamber which was irradiated with a beam of π^- mesons at 40 GeV/c. The distribution of rapidity-gap lengths between the secondary charged particles adjacent in rapidity is used which can help to decide whether the model due to Snider or QPT is in conformity with the experimental data. According to Snider, the rapidity-gap distribution in rapidity space for nondiffraction events asymptotically can be written in the form

$$\frac{dn}{dr} = Ae^{-Br} + Ce^{-Dr}, \quad (1)$$

where A , B , C , and D are constants. Snider predicted the values of constants as 2.4, 3.1, 0.2, and 0.9, respectively. On the other hand, QPT suggested the single-exponential form

$$\frac{dn}{dr} \simeq e^{-pr}$$

of rapidity-gap distribution (for large r). Another prediction of the Snider model was that preferably a small (large) gap is being repeated after a small (large) gap, whereas QPT suggest that these gaps tend to repeat alternately. In view of this, the decay products of the cluster would be more than two charged particles for the Snider model, in contrast to the model due to QPT, which suggests two charged particles as a size of the cluster. These are a few important outcomes of these two models which can be tested using rapidity gaps.

II. EXPERIMENTAL DETAILS

The experimental data used in the present investigation was collected by the JINR group using the two-meter bubble chamber bombarded by π^- mesons with momentum 40 GeV/c. The details about exposure, scanning, and measurements are give in Ref. 3. In accordance with the previously established criteria all of the events collected were classified as π^-p , π^-n , and π^-C and the number of events for these types of interactions are 11 170, 3940, and 5050, respectively.

III. RESULTS AND DISCUSSIONS

The rapidity variable is defined as

$$y = \frac{1}{2} \ln \frac{E + p_L}{E - p_L},$$

where E and p_L are the energy and longitudinal momentum, respectively, of a particle. As mentioned above, the analysis is based on the rapidity gap, which is defined as the difference in rapidity between neighboring final-state particles when par-

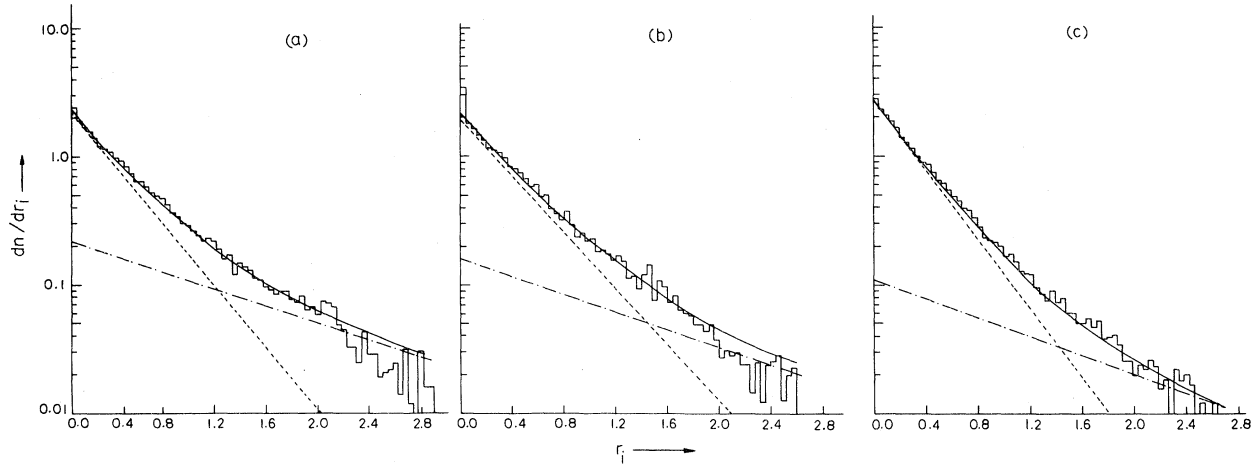


FIG. 1. The rapidity-gap (r_i) distribution for charged particles in (a) π^-p , (b) π^-n , and (c) π^-C collisions at 40 GeV/c. The dashed lines represent the contributions of two exponential terms individually.

ticles in each event are arranged in ascending order in terms of their rapidity. The highest and the lowest rapidity particles are not considered, in order to eliminate the contribution coming from diffraction dissociation.

Figures 1(a), 1(b), and 1(c) show the rapidity-gap distributions for π^-p , π^-n , and π^-C types of interactions. Strong peaks are clearly seen in all the three distributions for small values of rapidity gaps which indicates the existence of strong short-short correlation. It is also inferred from these figures that short-short correlation does exist in both π^- -nucleon and π^- -nucleus interactions as has been observed in pN and pA interactions.¹⁴ As is evident from the figures, the rapidity-gap distributions cannot be represented by a single exponential. These distributions for all three types of interactions can be well explained by a theoretical asymptotic form of type (1) and the least-squares fit to the data yields

$$\frac{dn}{dr_i} = (1.93 \pm 0.05)e^{-(2.53 \pm 0.13)r_i} + (0.16 \pm 0.06)e^{-(0.75 \pm 0.16)r_i}, \quad (2)$$

$$\frac{dn}{dr_i} = (2.67 \pm 0.03)e^{-(3.06 \pm 0.05)r_i} + (0.11 \pm 0.01)e^{-(0.85 \pm 0.06)r_i}, \quad (3)$$

$$\frac{dn}{dr_i} = (2.07 \pm 0.02)e^{-(2.76 \pm 0.05)r_i} + (0.22 \pm 0.02)e^{-(0.75 \pm 0.03)r_i} \quad (4)$$

for π^-p , π^-n , and π^-C interactions with $\chi^2/DF=71/73$, $76/72$, and $57/63$, respectively. The dashed lines in the figures show the contribution due to two individual terms in Eqs. (2)–(4). However, major contribution comes from the first term in all types of interactions. These results reveal that the model due to Snider is consistent with our experimental data. The slope D in Eq. (1) is generally referred to as cluster density. As seen from Eqs. (3) and (4) for π^-p and π^-n data at this energy the slopes B and D are slightly lower than those predicted by Snider, i.e., 3.1 and 0.9, respectively. But for π^-C interactions, the slopes are in agreement with Snider's prediction. The value of B is greater in π^-C interactions than in π^-N interactions; however, D is almost the same in the two types of interactions.

To get information about the short-short and short-long correlations in rapidity gaps we have studied the distribution of those gaps which are next to a small gap ($r_i \leq 0.1$). Figures 2(a), 2(b), and 2(c) exhibit these distributions for π^-p , π^-n , and π^-C interactions, respectively. The striking feature of the distributions is the strong peak for $r_i \leq 0.08$ which indicates that the probability of the occurrence of a small gap after a small gap is higher as compared to the occurrence of a large gap ($0.8 \leq r_i \leq 1.0$) after a small gap. From this it is evident that short-short correlation is dominant as compared to short-long correlation, and cluster size is more than two charged particles. This observation favors strongly the model by Snider. We have also obtained the ratio of small gaps ($r \leq 0.1$) and large gaps ($0.8 \leq r \leq 1.0$) in these distributions. This ratio is 6.2 ± 0.2 , 8.6 ± 0.9 , and 6.2 ± 0.6 for

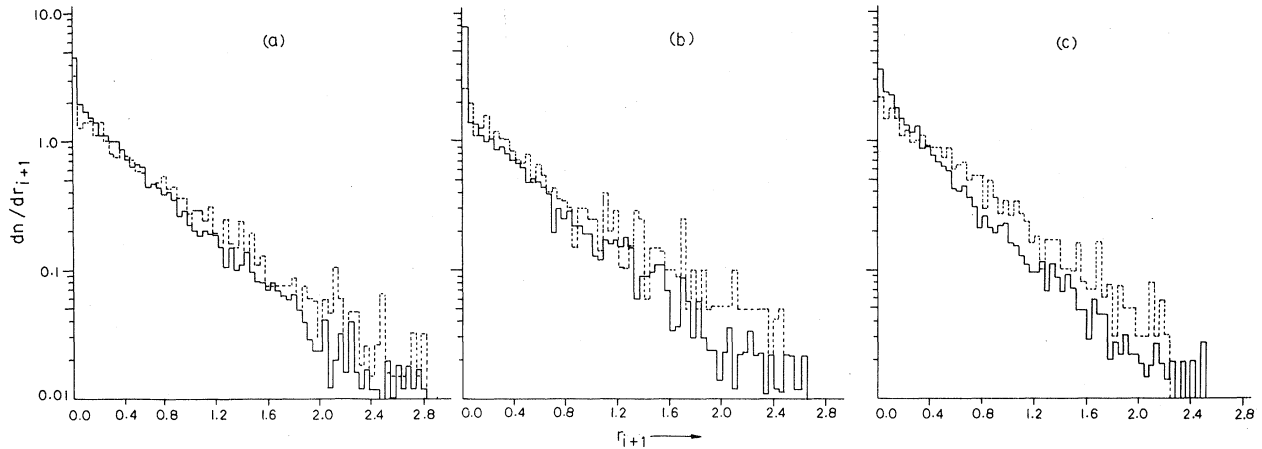


FIG. 2. The distributions of rapidity gap (r_{i+1}) in (a) π^-p , (b) π^-n , and (c) π^-C collisions at 40 GeV/c. The distributions represented by solid lines are due to the gap next to small gaps $r_i (r_i \leq 0.1)$. The distributions represented by dashed lines are due to the gap next to large gaps $r_i (0.8 \leq r_i \leq 1.0)$ normalized to the distribution represented by solid lines.

π^-p , π^-n , and π^-C interactions, respectively. A double exponential form of type (1) can also represent the distributions of small rapidity gaps for π^-p , π^-n , and π^-C types of interactions and corresponding best-fit equations were obtained as

$$\frac{dn}{dr_{i+1}} = (2.40 \pm 0.07)e^{-(3.13 \pm 0.14)r_{i+1}} + (0.18 \pm 0.04)e^{-(0.77 \pm 0.13)r_{i+1}}, \quad (5)$$

$$\frac{dn}{dr_{i+1}} = (2.74 \pm 0.08)e^{-(3.42 \pm 0.14)r_{i+1}} + (0.19 \pm 0.05)e^{-(0.87 \pm 0.13)r_{i+1}}, \quad (6)$$

$$\frac{dn}{dr_{i+1}} = (2.73 \pm 0.08)e^{-(3.40 \pm 0.14)r_{i+1}} + (0.16 \pm 0.03)e^{-(0.74 \pm 0.11)r_{i+1}}, \quad (7)$$

where $\chi^2/DF = 62/60$, $65/10$, and $57/60$, respectively. The comparison between Eqs. (2)–(4) and (5)–(7) suggests that the slope parameter D remains almost the same. However, this probability signifies that the probability of occurrence of a short gap next to a short gap is greater because otherwise the distribution of gaps adjacent to a short gap should have been similar to the original r distribution.

The study of long-short and long-long correlations in rapidity gaps has also been made and the distributions for the gaps next to a large gap have been depicted in Figs. 2(a), 2(b), and 2(c) for π^-p ,

π^-n , and π^-C types of interactions (dashed histograms). The distributions of gaps next to large gaps have been normalized to the distributions of gaps next to small gaps. The normalizing factors are 3.7, 4.5, and 5.5 for π^-p , π^-n , and π^-C interactions, respectively. One can notice the depletion in the distributions of gaps next to large gaps in comparison with the distributions of gaps next to small gaps in low values of r , while for large values of r the distributions are higher in the former case than in the latter. In these distributions also we have obtained the ratio of small gaps ($r \leq 0.1$) and large gaps ($0.8 \leq r \leq 1.0$). This ratio in π^-p , π^-n , and π^-C interactions is 3.5 ± 0.4 , 4.0 ± 0.9 , and 3.3 ± 0.5 , respectively. Comparing this ratio with the values of ratios obtained for the distribution of gaps next to small gaps we observe that these are half the earlier values. This implies that short-short correlation is more pronounced as compared to long-short correlation, at least by a factor of 2. One can notice from the figures that the long-long correlation effect is slightly more dominant than short-long correlation (see figures). It may be summarized that the long-short correlations occur in all types of high-energy interactions and the strength of this correlation is almost target-size independent, which might be due to the idea that different clusters produced in rapidity space are separated by large rapidity gaps and a short gap is followed by a short gap and a large gap is also followed by a short gap. The features of rapidity-gap correlations can occur, if in an event a number of clusters are produced and they have more than two charged particles.

According to Snider the ratio of the two plotted distributions, Figs. 1(a), 1(b), and 1(c) and Figs. 2(a), 2(b), and 2(c) at $r_i=2.0$, when normalized by their values at $r_i=0.0$, is 1.54, i.e.,

$$[f(2)/f(0)]/[g(2)/g(0)]=1.54,$$

where g and f represent the distribution of all rapidity gaps and the gaps next to small rapidity gaps, respectively. In this investigation this ratio for π^-p , π^-n , and π^-C interactions have been obtained to be 1.59 ± 0.03 , 1.60 ± 0.08 , and 1.49 ± 0.07 , respectively, which is again supporting the model due to Snider.

It is interesting to study the cluster size and cluster density in the rapidity space. The slope parameters B and D are used for this information. Adamovich *et al.*⁵ have deduced that the rapidity-gap distribution can be represented by

$$\frac{dn}{dr} = e^{-\rho mr} \quad (\text{for small } r),$$

$$\frac{dn}{dr} = e^{-\rho r} \quad (\text{for large } r),$$

where m denotes the cluster decay multiplicity and ρ indicates the cluster density. Comparing Eqs. (2)–(4), we obtained the values of m as 3.7 ± 0.2 , 3.4 ± 0.7 , and 3.6 ± 0.3 for π^-p , π^-n , and π^-C interactions, respectively. In the predictions of Snider also the value of m comes out to be 3.5 at 200

GeV for pp data which is clearly favored by our data. The values of m in p -Em interactions are 3.0 ± 0.4 , and 2.5 ± 0.6 at 400 and 200 GeV, respectively. Ludlam and Slansky also obtained the values of m to be 4.0 ± 0.8 at 205 GeV/ c and 3.5 ± 0.8 at 300 GeV/ c , by the fluctuation-analysis method.⁶ This indicated that cluster size remains independent of energy.

To conclude, we can say that the particle production takes place via clusters. Similar conclusions have been drawn in hadron-hadron, hadron-nucleus, and nucleus-nucleus collisions.⁷ However, it may be admitted that the rapidity-gap analysis as has been undertaken in this study may not be sensitive enough to determine the strength of clustering effects as it does not take account of long-range kinematic correlations.

As evidenced in this study, the clusters are intervened by large rapidity gaps. There are on an average more than two charged particles (maybe 3–4) per cluster and there are several clusters in one event. The decay products of the cluster remain almost independent of energy as well as target size in both hN and hA interactions.

The authors are indebted to the Directorate of the Joint Institute for Nuclear Research, Dubna, U.S.S.R. for sending the 40-GeV Data Summary Tape.

¹D. R. Snider, Phys. Rev. D **11**, 140 (1977); Report No. ILL-(IH)-75-5, 1975 (unpublished); G. F. Chew *et al.* Phys. Rev. **176**, 2112 (1968).

²C. Quigg, P. Piri la, and G. H. Thomas, Phys. Rev. Lett. **34**, 290 (1975).

³A. V. Abdurakhimov *et al.*, Phys. Lett. **39B**, 571 (1972); N. Angelov *et al.*, Yad. Fiz. **24**, 356 (1976) [Sov. J. Nucl. Phys. **24**, 186 (1976)]; and V. G. Grishin, private communication, 1979.

⁴M. M. Aggarwal *et al.*, J. Phys. Soc. Jpn. **51**, 2 (1981).

⁵M. I. Adamovich *et al.*, Nuovo Cimento **33A**, 183 (1976).

⁶T. Ludlam *et al.*, Phys. Lett. **48B**, 449 (1974).

⁷R. K. Shivpuri *et al.*, Nuovo Cimento **49A**, 67 (1979); Chandra Gupt and R. K. Shivpuri, Lett. Nuovo Cimento **26**, 88 (1979); P. L. Jain *et al.*, *ibid.* **26**, 9 (1979); S. Roy *et al.*, Phys. Rev. D **21**, 2497 (1980); N. S. Arya *et al.*, Prog. Theor. Phys. **63**, 939 (1980); M. M. Aggarwal *et al.*, J. Phys. Soc. Jpn. **51**, 2 (1981).